

ON THE STABILITY OF THE ROBOT COMPLIANT MOTION CONTROL
(INPUT OUTPUT APPROACH)

H. Kazerooni

Mechanical Engineering Department
University of Minnesota
Minneapolis, MN 55455

Abstract

The work presented here is a practical, nonlinear controller design methodology for robot manipulators. This methodology guarantees: 1) the robot end-point follows an input command vector "closely" when the robot is not constrained by the environment, and 2) the contact force is a function of the same input command vector (used in the unconstrained environment) when the robot is constrained by the environment. The controller is capable of "handling" both constrained and unconstrained maneuverings, and is robust to bounded uncertainties in the robot dynamics. The controller does not need any hardware or software switch for the transition between unconstrained and constrained maneuvering. Stability of the environment and the manipulator as a whole has been investigated, and a bound for stable manipulation has been derived.

Nomenclature

A the closed-loop mapping from r to f
d $n \times 1$ vector of the external force on the robot end-point
e $n \times 1$ input trajectory vector
 e_m, d_m positive scalars
E environment dynamics
f $n \times 1$ vector of the contact force
 f_∞ the limiting value of the contact force for rigid environment
G robot dynamics with positioning controller
H compensator transfer function matrix
r $n \times 1$ input-command vector
n degrees of the freedom of the system $n \leq 6$
S robot manipulator stiffness
T positive scalar
V the forward loop mapping from e to f
x environment deflection
y $n \times 1$ vector of the robot end-point position
 y_∞ the limiting value of the robot position for rigid environment
 x_0 $n \times 1$ vector of the environment position before contact
 θ $n \times 1$ vector of the joint angles of the robot

ϵ_s, ϵ_d positive scalars
 ω_0 frequency range of operation (bandwidth)
 α_1, β_1 positive scalars

1. Introduction

In general, manipulation consists of two categories. In the first category, the manipulator end-point is free to move in all directions. In the second, the manipulator end-point interacts mechanically with the environment. Most assembly operations and manufacturing tasks require mechanical interactions with the environment or with the object being manipulated, along with "fast" motion in free and unconstrained space. Therefore, the objective of this work is to develop a control system such that the robot will be capable of "handling" both types of maneuvers without any hardware and software switches. The hardware and software switches used in algorithms such as hybrid force/position control develop unpleasant transient response in the transition period. In meeting the above objective, the goal is to develop a controller for the robot manipulators such that:

- 1) The robot end-point follows an input-command vector "closely" when the robot is not constrained (a more rigorous definition for "closely" will follow).
- 2) The contact force¹ is a function of the same input-command used in the unconstrained maneuvering when the robot is constrained by the environment.

Previous researchers have suggested two approaches for assuring compliant motion for robot manipulators. The first approach is aimed at controlling force and position in a nonconflicting way. In this method, force is commanded along those directions constrained by the environment, while position is commanded along those directions in which the manipulator is unconstrained and free to move [11,12,13,19,20]. The second approach is aimed at developing a relationship between the interaction

forces and the manipulator position. By controlling the manipulator position and specifying its relationship to the interaction forces, one can ensure that the manipulator will be able to maneuver in a constrained environment while maintaining appropriate contact forces [1,3,4,14]. The design method presented here is considered to be part of the second approach toward developing compliant motion. We are looking for a controller that guarantees the tracking of the input command vector when the robot is not constrained, as well as the relation of the contact force vector with the same input command vector when the robot encounters an unknown environment.

Section 2 describes the points of importance in generating compliant motion. This will lead us to Section 3 that introduces the controller design specifications. Section 4 is devoted to describing a new approach in modeling the robot manipulators while Section 5 develops a method for modeling the environment. The architecture of the closed-loop control is presented in Section 7, and the stability of the closed loop system is analyzed in sections 8 and 9. Reference 8 describes an example of the application of this method on an active end-effector

2. Motivation

The following scenario reveals the crucial need for compliance control in high-speed manufacturing operations. Consider an assembly operation by a human worker in which there are parts to be assembled on the table. Each time the worker decides to reach the table and pick up a part, she/he always encounters the table with a non-zero speed; in other words she/he hits the table while picking up the parts. The worker also assembles the parts with a non-zero speed; meaning the parts hit each other while they are assembled. The ability of the human hand to encounter the unknown and unstructured environment with non-zero speed allows for a higher speed of operation. This ability in human beings flags the existence of a compliance control mechanism in biological systems. This mechanism guarantees the "stability" of contact forces in constrained maneuvering, in addition to high speed maneuvering in an unconstrained environment. With the existing state of technology, we do not have an integrated robotic assembly system that can encounter an unstructured environment as a human worker can. No existing robotic assembly system is faster than a human hand. The compliancy in the human hand allows the worker to encounter the environment with non-zero speed. The above example does not imply that we choose to imitate human factory-level physiological/

psychological behavior as our model to develop an overall control system for manufacturing tasks such as assembly and finishing processes. We stated this example to show that: 1) a reliable and optimum solution for simple manufacturing tasks such as assembly does not yet exist and 2) it is the existence of an efficient, fast compliance control system in human beings that allows for superior and faster performance. We believe compliance control is one of the key issues in the development of high-speed manufacturing operations for robot manipulators.

3. The Controller Design Objectives

The design objective is to provide a stabilizing dynamic compensator for the robot manipulator such that the following design specifications are satisfied.

- I. The robot end-point follows an input-command vector, r , when the robot manipulator is free to move.
- II. The contact force, f , is a function of the input command vector, r , when the robot is in contact with the environment.

The first design specification allows for free manipulation when the robot is not constrained. If the robot encounters the environment, then according to the second design specification, the contact force will be a function of the input command vector. Thus, the system will not have a large and uncontrollable contact force. Note that r is an input command vector that is used for both unconstrained and constrained maneuvers. The end-point of the robot will follow r when the robot is unconstrained, while the contact force will be a function of r (preferably a linear function for some bounded frequency range of r) when the robot is constrained.

4. Dynamic Model of the Robot with Positioning Controllers

In this section we develop a new general approach to describe the dynamic behavior of a large class of industrial and research robot manipulators having positioning controllers. The fact that most industrial manipulators have some kind of positioning controllers is the motivation behind our approach. Also, a number of methodologies exist for the development of the robust positioning controllers for direct and non-direct robot manipulators [15,18]. The unified approach of modeling robot dynamics presented here is expressed in terms of sensitivity functions. It allows us to incorporate the dynamic behavior of all the

elements of a robot manipulator (i.e. actuators, sensors and the links structural compliance) in addition to the rigid body dynamics.

Section 4.1 is devoted to the nonlinear time domain dynamic modeling of the robot manipulators while section 4.2 describes the frequency domain modeling of the robot manipulators. Although the frequency domain technique is confined to linear systems, it gives more insights to this general approach in modeling the dynamic behavior of the robot. Since inertia-invariant robot manipulators have linear dynamic behavior, it is more reasonable to use frequency domain techniques for controller design and analysis. The frequency domain design can also be used when the robot dynamics is linearized in the neighborhood of a particular trajectory.

4.1 Time-Domain, Nonlinear Dynamic Model of the Robot with Positioning Controllers

The end-point position of a robot manipulator that has a positioning controller is "approximately" equal to the input trajectory vector, e , if e is bounded in magnitude. The approximate equality of e and the actual end-point position (in absence of external force on the robot end-point) can be represented by mapping G in equation 1.

$$y = G(e) \quad (1)$$

$$\text{where: } \frac{\|y - e\|_p}{\|e\|_p} < \epsilon_e \text{ for } \|e\|_p < e_m \quad (2)$$

e : The n -dimensional ($n \leq 6$) input trajectory vector in a global cartesian coordinate frame.

y : The n -dimensional ($n \leq 6$) position vector of the robot end-point in a global cartesian coordinate frame.

The definition for $\|\cdot\|_p$ (P-norm) is given in Appendix A. Note that e is the input trajectory vector that a commercial robot manipulator accepts via its positioning controller. Because of limitation on the size of the actuator torque, one cannot track a "large" trajectory vector, e , with a small error, ϵ_e . Scalar e_m is defined to represent the confinement of the norm ("magnitude" in the multivariable sense) of e . One can always find an e_m and ϵ_e experimentally (or analytically if possible) for a particular robot manipulator.

Robot manipulators with positioning controllers are not infinitely stiff in response to external forces (also called disturbances). Even though the positioning controllers of robots are usually designed to follow the trajectory commands (according to relationships 1

and 2) and reject disturbances, the robot end-point moves somewhat in response to imposed forces on the robot end-point. The motion of the robot end-point in response to imposed forces is caused by either structural compliance in the robot or the positioning controller compliance. The motion of the end-point of a robot under the imposed force at the end-point, d , in the absence of any input trajectory vector can be represented by mapping S in equation 3.

$$y = S(d) \quad (3)$$

$$\text{where: } \frac{\|y\|_p}{\|d\|_p} < \epsilon_d \text{ for } \|d\|_p < d_m \quad (4)$$

d is the n -dimensional vector of the external force that is imposed on the robot end-point. The general form of the nonlinear dynamic equations of a robot manipulator with positioning controller can be given by two nonlinear vector functions G and S in equation 5. Note that although we have assumed d and e affect the robot in a nonlinear fashion, equation 5 assumes that the motion of the robot end-point is a linear addition of both effects.

$$y = G(e) + S(d) \quad (5)$$

The assumption that linear superposition holds for the effects of d and e is useful in understanding the nature of the interaction between the robot and the environment. This interaction is in a feedback form and will be clarified with the help of Figure 3. We will note in Section 6 that the results of the nonlinear analysis do not depend on this assumption and one can extend the obtained results to cover the case when $G(e)$ and $S(d)$ do not superimpose. Figure 1 shows the nature of the mapping in equation 5. No assumption on the internal structures of $G(e)$ and $S(d)$ are made. We assume that $G(e)$ and $S(d)$ are stable, nonlinear operators in the L_p -space; in other words $G(e)$ and $S(d)$ are such that $G: L_p^n \rightarrow L_p^n$, $S: L_p^n \rightarrow L_p^n$ and also there exist constants α_1 , β_1 , α_2 , and β_2 such that $\|G(e)\|_p < \alpha_1 \|e\|_p + \beta_1$ and $\|S(d)\|_p < \alpha_2 \|d\|_p + \beta_2$. (The definition of stability in L_p -sense is given in Appendix A)

The modeling method described here allows us to represent an approximation of the dynamic behavior of the closed-loop positioning robot. This occurs without being specific about the nature of the input trajectory, e , and the structure of the positioning controller. A similar modeling method is given in Section 4.2 for analysis of the linearly treated robots.

4.2 Frequency Domain Dynamic Model of the Robot with Positioning Controllers

A transfer function matrix, G , in equation 6 is

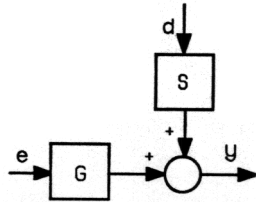
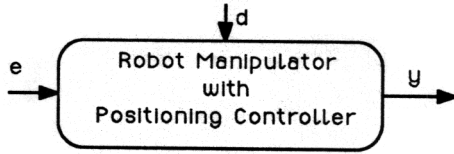


Figure 1: The Dynamic of the Manipulator with the Positioning Controller

defined to describe the dynamic behavior of a robot manipulator with positioning controller. This transfer function matrix maps the amplitude of the input trajectory, e , to the amplitude of the robot trajectory, y .

$$y(j\omega) = G(j\omega) e(j\omega) \quad (6)$$

where:

$$\frac{\|(G(j\omega) - I_n)e(j\omega)\|_2}{\|e(j\omega)\|_2} < \epsilon_e \quad (7)$$

for all $\omega \in \omega_o$ and $\|e\|_2 < e_m$

Some explanations are needed for the practical conditions that are imposed by e_m and ω_o on inequality 7. Because of the limitation on the size of the actuator torque, one cannot track a "large" input trajectory, e , with a small tracking error, ϵ_e , within the frequency range of $[0, \omega_o]$. Scalar e_m is defined to represent the confinement of the magnitude of e . Physical systems are not responsive to high frequency input trajectory commands. Inequality 7 will not hold at high frequencies. ω_o is introduced to represent this limitation. The frequency range $[0, \omega_o]$ where inequality 7 holds, is called the bandwidth of the closed-loop positioning system [2,6]. ϵ_e is a small number for good positioning systems. As an example, for the ADEPT robot, ϵ is equal to 0.01 for all $\|e\|_2 < 1$ cm, and $\omega \in [0, 5]$ hertz. With any type of positioning controller, one can always arrive at inequality 7 experimentally or analytically. Conservative values for ω_o and e_m are adequate to represent an approximation of the closed-loop positioning dynamic for the robot.

We express the dynamic behavior of a robot manipulator in response to forces on the robot end-point similarly. We can express the sensitivity of a robot manipulator by a matrix, S . The motion of the end-point of a robot under the imposed force, d , at the end-point, in the absence of any input trajectory vector can be given by equation 8.

$$y(j\omega) = S(j\omega) d(j\omega) \quad (8)$$

$$\frac{\|S(j\omega) d(j\omega)\|_2}{\|d(j\omega)\|_2} < \epsilon_e \quad (9)$$

for all $\omega \in \omega_o$ and $\|d\|_2 < d_m$

S is a transfer function matrix that represents the compliance (1/stiffness) of the robot. S is called the sensitivity matrix and for "good" positioning systems is quite "small". (By "small" we mean the maximum singular value² of S is a small number for all the frequencies for which the external force, d affects the system.)

Assuming that the motion of the robot end-point is a linear addition of e and d , equation 10 can be written to represent the dynamic behavior of a linearly treated robot with a positioning controller:

$$y(j\omega) = G(j\omega)e(j\omega) + S(j\omega)d(j\omega) \quad (10)$$

In the case of robot manipulators with linearized dynamics in the neighborhood of a particular trajectory, $G(\theta_o, j\omega)$ and $S(\theta_o, j\omega)$ - where θ_o represents the robot operating point - are more formal representatives of the robot dynamics.

5. Dynamic Behavior of the Environment

There is no specific model for the environment dynamics. The environment can be very "soft" or very "hard". We do not restrain ourselves to any geometry or to any structure. We try to avoid using structured dynamic models such as first or second order transfer functions or mass and spring systems as general representation of the dynamic behavior of the environment. These models are not general and the stability analysis consequently results in non-general conclusions. Section 5.1 is devoted to nonlinear time-domain dynamic analysis of the environment while section 5.2 develops a linear dynamic behavior of the environment in frequency domain.

5.1 Nonlinear, Time Domain Dynamic Behavior of the Environment

We assume that if one point on the surface of the environment is displaced (e.g. by the end-point of the robot) as vector of x , then the required force to do such a task is defined by f (Figure 2). Mapping E in equation 10 represents the dynamic behavior of the environment.

$$f = E(x) \quad (11)$$

x_o is the the initial location of the point of contact before deformation occurs and y is the robot end-point position ($x = y - x_o$). No assumption is made on the structure of E . We also assume E is stable in L_p -sense;

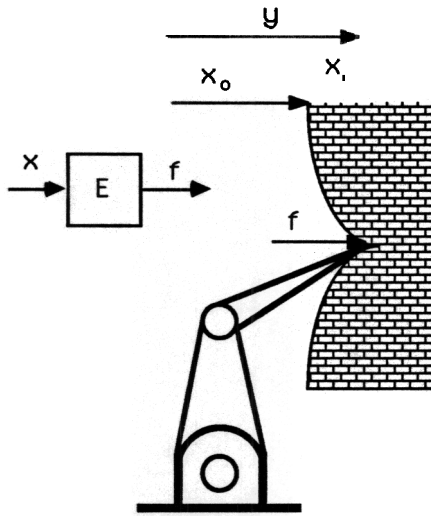


Figure 2: The Environment and Its Dynamics

$E: L_p^n \rightarrow L_p^n$ and also there exist constants such as α_3 and β_3 such that $\|E(x)\|_p < \alpha_3 \|x\|_p + \beta_3$.

5.2 Dynamic Behavior of the Environment in Frequency Domain

Extending equation 11 to cover the linearly treated environment, equation 12 represents the dynamic behavior of the environment with linear differential equations.

$$f(j\omega) = E(j\omega) x(j\omega) \quad (12)$$

$E(j\omega)$ is a transfer function matrix that maps the amplitude of the displacement vector, x to the amplitude of the contact force, f . The matrix E is a $n \times n$ transfer function matrix. No assumption about E is made; E is a singular matrix when the robot interacts with the environment in only some directions. For example, in grinding a surface, the robot is constrained by the environment in the direction normal to the surface only. Readers can be convinced of the truth of equation 12 by analyzing the relationship of the force and displacement of a spring as a simple model of the environment. E resembles the stiffness of a spring. Reference 3 and 4 represent $(Ms^2 + Cs + K)$ for E where M , C and K are symmetric square matrices and $s = j\omega$. M is the positive definite inertia matrix while C and K are the damping and the stiffness matrices.

6. Nonlinear Dynamic Behavior of the Robot Manipulator and Environment

Suppose a manipulator with dynamic equation 5 is in contact with an environment given by equation 11. The contact force will be equal to f . Note that when the robot manipulator and environment are in contact with each other, $f = -d$ and $x = y - x_0$. Figure 3 shows the dynamics of the robot manipulator and the

environment when they are in contact with each other. Note that in some applications, the robot will have only uni-directional force on the environment. For example, in the grinding of a surface by a robot, the robot can only push the surface. If one considers positive f_i for "pushing" and negative f_i for "pulling", then in this class of manipulation, the robot manipulator and the environment are in contact with each other only along those directions where $f_i > 0$ for $i = 1, \dots, n$. In some applications such as screwing a bolt, the interaction force can be positive and negative. This means the robot can have clockwise and counter-clockwise interaction torque. The nonlinear discriminator block-diagram in Figure 3 is drawn with dashed-line to illustrate the above concept.

Considering equations 5 and 11, equations 13 and 14 represent the entire dynamic behavior of the robot and environment as a whole.

$$\begin{aligned} y &= G(e) + S(-f) \\ f &= E(x) \quad \text{where } x = y - x_0 \end{aligned} \quad (14)$$

The block diagram in Figure 3 shows the nature of mappings 13 and 14.

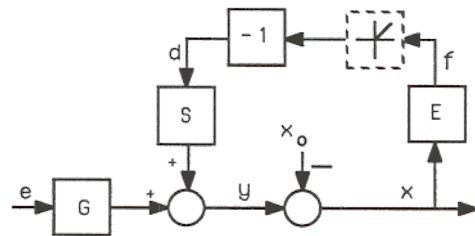


Figure 3: Interaction of the Robot Manipulator with the Environment

If all the operators in Figure 3 are considered linear transfer function matrices, equations 15 and 16 can be obtained from equations 13 and 14 to represent the end point position and the contact force when $x_0 = 0$.

$$y = (I + SE)^{-1} G e \quad (15)$$

$$f = E(I + SE)^{-1} G e \quad (16)$$

Equations 13 and 14 (equations 15 and 16 in the case of linearly treated robots) represent the dynamic behavior of the robot for both constrained and unconstrained manipulations. When the robot is not in contact with the environment, $x = 0$ and the equation that governs the dynamics of the system is given by equation 1 (equation 6 for the linearly treated robots). Note the natural feedback in the system; the force developed in the system from the interaction of the robot manipulator and the environment affects the robot motion in a feedback fashion.

To simplify our analysis, V is introduced in equation 17 as a mapping from e to f in Figure 3.

$$f=V[e] \quad (17)$$

The mappings given by equations 13 and 14 can be simplified by mapping $V:e \rightarrow f$ where e and f are shown in Figure 4. Note that V is assumed as stable operator in L_p -sense; in other words: $V:L_p^n \rightarrow L_p^n$ and also $\|V(e)\|_p < \alpha_4 \|e\| + \beta_4$ where α_4 and β_4 are constants. Note that one can still define V without assuming the superposition of effects of e and d in equation 5. If all the operators in Figure 3 are transfer function matrices, then $V=E(I+SE)^{-1}G$

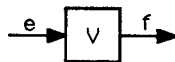


Figure 4: The Mapping from the Trajectory to the Contact Force

7. The Architecture of the Closed-loop System

The control architecture in Figure 5 shows how compliancy is being developed in the system. The motivation behind this architecture is clarified in Section 9 with the help of some equations. The compensator, H is considered to operate on the contact force, f . The compensator output signal is being subtracted from the input command vector, r , resulting in the error signal, e for the robot manipulator.

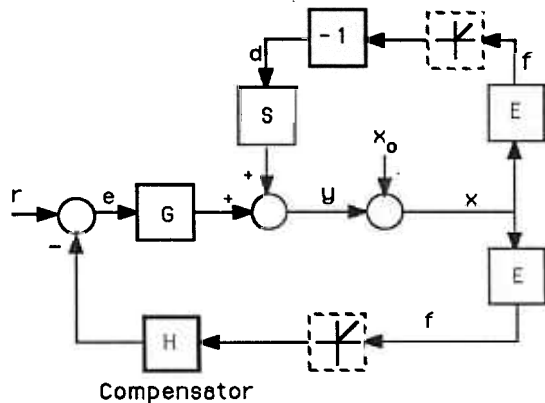


Figure 5: The Closed-loop System

There are two feedback loops in the system; the upper loop (which is the natural feedback loop), is the same as the one shown in Figure 3. This loop shows how the contact force affects the robot in a natural way when the robot is in contact with the environment. The lower feedback loop is the controlled feedback loop.

If the robot and the environment are not in contact, then the dynamic behavior of the system reduces to the one represented by equation 1, which is a simple positioning system. When the robot and the

environment are in contact, then the value of the contact force and the end-point position of robot are given by f and y where the following equations are true:

$$y=G(e)+S(-f) \quad (18)$$

$$f=E(x) \quad \text{where } x=y-x_0 \quad (19)$$

$$e=r-H(f) \quad (20)$$

If the operators in equations 18,19 and 20 are considered transfer function matrices, equations 21 and 22 can be obtained to represent the interaction force and the robot end point trajectory when $x_0=0$.

$$f=E(I+SE+GHE)^{-1}Gr \quad (21)$$

$$y=(I+SE+GHE)^{-1}Gr \quad (22)$$

We plan to choose a class of compensators, H , to control the contact force with the input command r . By knowing S , G and E and choosing H one can shape the contact force. The value of the H is the designer choice and depending on the task, it can have various values in different directions. A large value for H develops a compliant system while a small H generates a stiff system. H must also guarantee the stability of the closed-loop system of Figure 5. The trade-off between the closed-loop stability and the size of H is investigated in Sections 8 and 9.

When the robot is not in contact with the environment, the actual position of the robot end-point is governed by equation 1. When the robot is in contact with the environment, then the contact force follows r according to equations 18, 19 and 20. The input command vector, r , is used differently for the two categories of maneuverings; as an input trajectory command in unconstrained space (equation 1) and as a command to control force in constrained space. We do not command any set-point for force as we do in admittance control (13,19). This method is called Impedance Control (1,3,4) because it accepts a position vector as input and it reflects a force vector as output. There is no hardware or software switch in the control system when the robot travels from unconstrained space to constrained space. The feedback loop on the contact force closes naturally when the robot encounters the environment.

Section 8 is devoted to derivation of a sufficient condition for closed stability of the system in Figure 5, when all the operators are nonlinear mappings. Section 9 develops similar results when all the operators of Figure 5 are linear transfer function matrices. We also show that the stability condition derived in the linear frame is a subclass of the

condition derived by the nonlinear analysis.

8. Nonlinear Time Domain Stability Analysis

The objective of this section is to arrive at a sufficient condition for stability of the system shown in Figure 5. This sufficient condition leads to the introduction of a class of compensators, H, that can be used to develop compliancy for the family of robot manipulators with dynamic behavior represented by equation 5. Using operator V defined by equation 17, the block diagram of Figure 6 is constructed as a simplified version of the block diagram of Figure 5. The following theorem (Small Gain Theorem) states the stability condition of the closed-loop system shown in Figure 6. A corollary is then followed to represent a bound on H to guarantee the stability of the system.

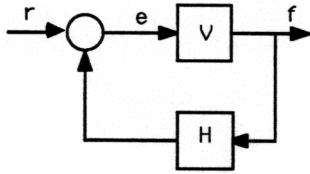


Figure 6: Manipulator and the Environment with Force Feedback Compensator (Simplified Version of Figure 5)

Stability Theorem.

If:

I. V is a L_p -stable operator, that is

$$a) \quad V(e): L_p^n \rightarrow L_p^n \quad (23)$$

$$b) \quad \|V(e)\|_p < \alpha_4 \|e\|_p + \beta_4 \quad (24)$$

where α_4 and β_4 are positive constants, and if

II. H is chosen such that mapping HV(e) is L_p -stable, that is

$$a) \quad HV(e): L_p^n \rightarrow L_p^n \quad (25)$$

$$b) \quad \|HV(e)\|_p < \alpha_5 \|e\|_p + \beta_5 \quad \text{where } \alpha_5 < 1 \quad (26)$$

then the closed-loop system (Figure 6) is L_p -stable.

Condition I is already assumed in Section 6. The Proof is given in Appendix A.

Corollary

The key parameter in the theorem is the size of α_5 . According to the above theorem, to guarantee the closed-loop stability of the system, H must be chosen such that the norm of HV(e) is linearly bounded with a slope that is smaller than unity. We choose H as a transfer function matrix, therefore inequality 27 is true.

$$\|HV(e)\|_p < \sigma_{\max}(H) \times \|V(e)\|_p \quad (27)$$

where $\sigma_{\max}(H)$ is the maximum singular value of H over all $\omega \in [0, \infty)$. Considering inequality 24, inequality 28 is

true.

$$\|HV(e)\|_p < \sigma_{\max}(H) \times (\alpha_4 \|e\|_p + \beta_4) \quad (28)$$

Comparing inequality 26 with inequality 28, to guarantee the closed-loop stability, $\sigma_{\max}(H) \alpha_4$ must be smaller than unity, or, equivalently:

$$\sigma_{\max}(H) < 1/\alpha_4 \quad (29)$$

Substituting for α_4 from inequality 24:

$$\sigma_{\max}(H) < 1/\alpha_4 < \frac{\|e\|_p}{\|V(e)\|_p - \beta_4} \quad (30)$$

To guarantee the stability of the closed-loop system, one sufficient for stability is can be obtained by considering $\beta_4 = 0$

$$\sigma_{\max}(H) < \frac{\|e\|_p}{\|V(e)\|_p}$$

To guarantee the stability of the closed-loop system, the $\sigma_{\max}(H)$ must be less than the reciprocal of the "magnitude" of the mapping in the forward loop in Figure 6. A similar result is given in Section 9 using multivariable Nyquist Criteria.

9. Frequency Domain Stability Analysis

The objective of this section is to arrive at a sufficient condition for stability of the system shown in Figure 5 when all the operators are linear transfer function matrices. This sufficient condition leads to the introduction of a class of transfer function matrices H, that stabilizes the family of linearly treated robot manipulators and environment with dynamic equations 11 and 12. The detailed derivation for the stability condition is given in Appendix C. According to the results of Appendix C, the sufficient condition for stability is given by inequality 32.

$$\sigma_{\max}(GHE) < \sigma_{\min}(SE + I_n) \quad \text{for all } \omega \in [0, \infty) \quad (32)$$

or a more conservative condition,

$$\sigma_{\max}(H) < \frac{1}{\sigma_{\max}(E(SE + I_n)^{-1}G)} \quad \text{for all } \omega \in [0, \infty) \quad (33)$$

If H is chosen outside of this class, instability and consequent separation may occur. Inequality 33 is a sufficient condition for stability. If inequality 33 is not satisfied, no conclusion on the stability of the system can be achieved. Note the similarity of the frequency domain stability condition with the one obtained by inequality 31. Substituting $E(SE + I_n)^{-1}G$ for V in inequality 31 and using the notation of singular values when $p=2$, inequality 33 will result. According to

Inequality 33, the "size" of H in all directions must be smaller than the reciprocal of the maximum "size" of the forward loop transfer function, $E(SE+I_n)^{-1}G$.

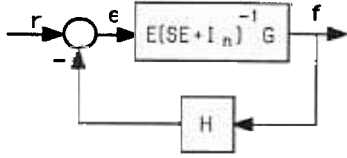


Figure 7: The Simplified Form of Figure 5

Inequality 33 reveals some facts about the size of H. The smaller the sensitivity of the robot manipulator is, the smaller H must be chosen. Also from Inequality 33, the more rigid the environment is, the smaller H must be chosen. In the "ideal case", no H can be found to allow a perfect positioning system ($S=0$) to interact with an infinitely rigid environment ($E=\infty$).

9.1 Stability for very rigid environment

In most manufacturing tasks such as robotic deburring, the end-point of the robot manipulator is in contact with a very stiff environment. Robotic deburring and grinding are examples of practical tasks in which the robot is in contact with hard environment [5,7,8]. According to the results in Appendix B, when the environment is very stiff, [E is very "large" in the singular value sense], the limiting value for the contact force and the end-point position are given by equations 34 and 35 respectively:

$$f_{\infty} = (S+GH)^{-1}G r \quad (34)$$

$$y_{\infty} = 0 \quad (35)$$

Since $G \approx I_n$ for all $\omega \in [0, \omega_0]$, the value of the contact force, f, within the bandwidth of the system $[0, \omega_0]$ can be approximated by equation 36:

$$f_{\infty} \approx (S+H)^{-1}r \quad \text{for all } \omega \in [0, \omega_0] \quad (36)$$

By knowing S and choosing H, one can shape the contact force. The value of $(S+H)$ within $[0, \omega_0]$ is the designer's choice and, depending on the task, it can have various values in different directions [3,4]. A large value for $(S+H)$ within $[0, \omega_0]$ develops a compliant system while a small $(S+H)$ generates a stiff system. If H is chosen such that $(S+H)$ is "large" in the singular value sense at high frequencies, then the contact force in response to high frequency components of r will be small. If H is chosen to guarantee the compliance in the system according to equation 34, then it must also satisfy the stability condition. It can be shown that the stability criteria for interaction with a very rigid environment is given by inequality 37:

$$\sigma_{\max}(H) < \frac{1}{\sigma_{\max}(S^{-1}G)} \quad \text{for all } \omega \in [0, \infty) \quad (37)$$

It is clear that if the environment is very rigid, then one must choose a very small H to satisfy the stability of the system when S is "small". [A good positioning system has "small" S]. Since $G \approx I_n$ for all $\omega \in [0, \omega_0]$, the bound for H, for a rigid environment and a "small" stiffness, is given by inequality 38.

$$\sigma_{\max}(H) < \sigma_{\min}(S) \quad \text{for all } \omega \in [0, \omega_0] \quad (38)$$

If S is zero, then no H can be obtained to stabilize the system. In other words to stabilize the system of the very rigid environment and the robot, there must be a minimum compliancy in the robot.

9.2 Stability Condition when $n=1$

In the case of the one degree of freedom system in Figure 8 the condition for stability is given by inequality 39.

$$\|HG\|_2 < \|(S+1/E)\|_2 \quad \text{for all } \omega \in [0, \infty) \quad (39)$$

where $\|\cdot\|$ denotes the magnitude of a transfer function. Since in many cases $G \approx 1$ for all $0 < \omega < \omega_0$, then H must be chosen such that the following inequality is satisfied.

$$\|H\|_2 < \|(S+1/E)\|_2 \quad \text{for all } \omega \in [0, \omega_0] \quad (40)$$

Inequality 39 clearly shows that the more rigid the environment is, the smaller H must be chosen to guarantee the stability of the closed-loop system. In the case of a rigid environment ("large" E) and a "good" positioning system, H must be chosen as a very small gain.

We conclude that for stability of the environment and the robot taken as a whole, there must be some initial compliancy either in the robot or in the environment. The initial compliancy in the robot can be obtained by a non-zero sensitivity function or a passive compliant element such as an RCC (Remote Center Compliance). Practitioners always observed that the system of a robot and a stiff environment can always be stabilized when a compliant element (e.g. piece of rubber or an RCC) is installed between the robot and environment. One can also stabilize the system of robot and environment by increasing the robot sensitivity function. In many commercial manipulators the sensitivity of the robot manipulators can be increased by decreasing the gain of each actuator positioning loop. This also results in a narrower bandwidth (slow response in the unconstrained maneuvering) for the

robot positioning system.

10. Summary and Conclusion

A new controller architecture for compliance control has been investigated using unstructured models for dynamic behavior of robot manipulators and environment. This unified approach of modeling robot and environment dynamics is expressed in terms of sensitivity functions. The control approach allows not only for tracking the input-command vector, but also for compliancy in the constrained maneuverings. A bound for the global stability of the manipulator and environment has been derived. For stability of the environment and the robot taken as a whole, there must be some initial compliancy either in the robot or in the environment. The initial compliancy in the robot can be obtained by a non-zero sensitivity function or a passive compliant element such as an RCC (Remote Center Compliance).

Appendix A

Definitions 1 to 7 will be used in the stability proof of the closed-loop system [16,17].

Definition 1: For all $p \in (1, \infty)$, we label as L_p^n the set consisting of all functions $f = (f_1, f_2, \dots, f_n)^T: [0, \infty) \rightarrow \mathbb{R}^n$ such that:

$$\int_0^{\infty} |f_i|^p dt < \infty \quad \text{for } i = 1, 2, \dots, n$$

Definition 2: For all $T \in [0, \infty)$, the function f_T defined by:

$$f_T = \begin{cases} f & 0 \leq t \leq T \\ 0 & T < t \end{cases}$$

is called the truncation of f to the interval $[0, T]$.

Definition 3: The set of all functions $f = (f_1, f_2, \dots, f_n)^T: [0, \infty) \rightarrow \mathbb{R}^n$ such that $f_T \in L_p^n$ for all finite T is denoted by L_{pe}^n . f by itself may or may not belong to L_p^n .

Definition 4: The norm on L_p^n is defined by:

$$\|f\|_p = \left(\sum_{i=1}^n \|f_i\|_p^2 \right)^{1/2}$$

where $\|f_i\|_p$ is defined as:

$$\|f_i\|_p = \left(\int_0^{\infty} w_i |f_i|^p dt \right)^{1/p}$$

where w_i is the weighting factor. w_i is particularly useful for scaling forces and torques of different units.

Definition 5: Let $V(\cdot): L_{pe}^n \rightarrow L_{pe}^n$. We say that the operator $V(\cdot)$ is L_p -stable, if:

a) $V(\cdot): L_{pe}^n \rightarrow L_{pe}^n$

b) there exist finite real constants α_4 and β_4 such that

$$\|V(e)\|_p < \alpha_4 \|e\|_p + \beta_4 \quad \forall e \in L_{pe}^n$$

According to this definition we first assume that the operator maps L_{pe}^n to L_{pe}^n . It is clear that if one does not show that $v(\cdot): L_{pe}^n \rightarrow L_{pe}^n$, the satisfaction of condition (a) is impossible since L_{pe}^n contains L_p^n . Once the mapping, $v(\cdot)$, from L_{pe}^n to L_{pe}^n is established, then we say that the operator $v(\cdot)$ is L_p -stable if, whenever the input belongs to L_p^n , the resulting output belongs to L_p^n . Moreover the norm of the output is no larger than α_4 times the norm of the input plus the offset constant β_4 .

Definition 6: The smallest α_4 such that there exist a β_4 so that inequality b of Definition 5 is satisfied is called the gain of the operator $v(\cdot)$.

Definition 7: Let $V(\cdot): L_{pe}^n \rightarrow L_{pe}^n$. The operator $V(\cdot)$ is said to be causal if:

$$V(e)_T = V(e_T) \quad \forall T < \infty \quad \text{and} \quad \forall e \in L_{pe}^n$$

Proof of the stability theorem

Define the closed-loop mapping $A: r \rightarrow e$ (Figure 6).

$$e = r - HV(e) \tag{A1}$$

For each finite T , inequality A2 is true.

$$\|e_T\|_p < \|r_T\|_p + \|HV(e)_T\|_p \quad \text{for all } t \in [0, T]$$

Since $HV(e)$ is L_p -stable. Therefore, inequality A3 is true.

$$\|e_T\|_p < \|r_T\|_p + \alpha_5 \|e_T\|_p + \beta_5 \quad \text{for all } t \in [0, T] \tag{A3}$$

Since α_5 is less than unity:

$$\|e_T\|_p < \frac{\|r_T\|_p}{1 - \alpha_5} + \frac{\beta_5}{1 - \alpha_5} \quad \text{for all } t \in [0, T]$$

Inequality A4, shows that $e(\cdot)$ is bounded over $[0, T]$. Because this reasoning is valid for every finite T , it follows that $e(\cdot) \in L_{pe}^n$, i.e., that $A: L_{pe}^n \rightarrow L_{pe}^n$. Next we show that the mapping A is L_p -stable in the sense of definition 5. Since $r \in L_p^n$, therefore $\|r\|_p < \infty$ for all $t \in [0, \infty)$, therefore inequality A5 is true.

$$\|e\|_p < \infty \quad \text{for all } t \in [0, \infty)$$

inequality A5 implies e belongs to L_p -space whenever r belong to L_p -space. With the same reasoning from

equations A1 to A5, it can be shown that inequality A6 is true.

$$\|e\|_p < \frac{\|r\|_p}{\beta_5} + \frac{\beta_5}{\beta_5} \quad (A6)$$

Inequality A6 shows the linear boundedness of e . (Condition b of definition 5) Inequality A6 and A5 taken together, guarantee that the closed-loop mapping A is L_p -stable.

Appendix B

A very rigid environment generates a very large force for a small displacement. We choose the minimum singular value of E to represent the size of E . The following theorem states the limiting value of the force when the robot manipulator is in contact with a very rigid environment.

Theorem

If $\sigma_{\min}(E) > M$, where M is an arbitrarily large number, then the value of the force given by equation 21 will approach to the expression given by equation B1

$$f_{\infty} = (S+GH)^{-1} G r \quad (B1)$$

Proof: We will prove that $\|f_{\infty}-f\|_2$ approaches a small number as M approaches a large number.

$$f_{\infty} - f = (S+GH)^{-1} [I_n - (S+GH)^{-1} E (I_n + SE + GHE)^{-1}] G r \quad (B2)$$

Factoring $(I_n + SE + GHE)^{-1}$ to the right hand side:

$$f_{\infty} - f = (S+GH)^{-1} (I_n + SE + GHE)^{-1} G r \quad (B3)$$

$$\|f_{\infty} - f\|_2 < \sigma_{\max}[(S+GH)^{-1}] \times \sigma_{\max}[(I_n + SE + GHE)^{-1}] \times \sigma_{\max}(G) \|r\|_2 \quad (B4)$$

$$\|f_{\infty} - f\|_2 < \frac{\sigma_{\max}(G) \|r\|_2}{\sigma_{\min}(S+GH) \times [\sigma_{\min}(SE + GHE) - 1]} \quad (B5)$$

$$\|f_{\infty} - f\|_2 < \frac{\sigma_{\max}(G) \|r\|_2}{\sigma_{\min}(S+GH) \times [\sigma_{\min}(S+GH) \times \sigma_{\min}(E) - 1]} \quad (B6)$$

$\sigma_{\max}(G)$ and $\sigma_{\min}(S+GH)$ are bounded values. If $\sigma_{\min}(E) > M$, then it is clear that the left hand side of inequality B6 can be an arbitrarily small number by choosing M to be a large number. The proof for $y_{\infty} \approx 0$ is similar to the above.

Appendix C

The objective is to find a sufficient condition for stability of the closed-loop system in Figure 5 by Nyquist Criteria. The block diagram in Figure 5 can be reduced to the block diagram in Figure C1 when all the operators are linear transfer function matrices and $x_0 = 0$

There are two elements in the feedback loop; GHE

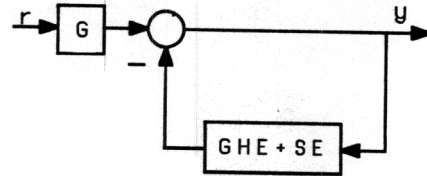


Figure C1: Simplified Block-Diagram of the System in Figure 5

and SE. SE shows the natural force feedback while GHE represents the controlled force feedback in the system. If $H=0$, then the system in Figure C1 reduces to the system in Figure 3 (a stable positioning robot manipulator which is in contact with the environment E .) The objective is to use Nyquist Criteria (10) to arrive at the sufficient condition for stability of the system when $H=0$. The following conditions are regarded:

- 1) The closed loop system in Figure C1 is stable if $H=0$. This condition simply states the stability of the robot manipulator and environment when they are in contact. (Figure 3 shows this configuration.)
- 2) H is chosen as a stable linear transfer function matrix. Therefore the augmented loop transfer function $(GHE+SE)$ has the same number of unstable poles that SE has. Note that in many cases SE is a stable system.
- 3) Number of poles on $j\omega$ axis for both loop SE and $GHE+SE$ are equal.

Considering that the system in Figure C1 is stable when $H=0$, we plan to find how robust the system is when HE is added to the feedback loop. If the loop transfer function SE (without compensator, H) develops a stable closed-loop system, then we are looking for a condition on H such that the augmented loop transfer function $(GHE+SE)$ guarantees the stability of the closed-loop system. According to the Nyquist Criteria, the system in Figure C1 remains stable if the clockwise encirclement of the $\det(SE+GHE+I_n)$ around the center of the S -plane is equal to the number of unstable poles of the loop transfer function $(SE+GHE)$. According to conditions 2 and 3, the loop transfer functions SE and $(SE+GHE)$ both have the same number of unstable poles. The closed-loop system when $H=0$ is stable according to condition 1; the encirclements of $\det(SE+I_n)$ is equal to unstable poles of SE. When H is added to the system, for stability of the closed-loop system, the number of the encirclements of $\det(SE+GHE+I_n)$ must be equal to the number of unstable poles of the $(SE+GHE)$. Since the number of unstable poles of $(SE+GHE)$ and SE are the same, therefore for stability of the system $\det(SE+GHE+I_n)$ must have the same number of encirclements that

$\det(SE+I_n)$ has. A sufficient condition to guarantee the equality of the number of encirclements of $\det(SE+GHE+I_n)$ and $\det(SE+I_n)$ is that the $\det(SE+GHE+I_n)$ does not pass through the origin of the s-plane for all possible non-zero but finite values of H, or

$$\det(SE+GHE+I_n) \neq 0 \quad \text{for all } \omega \in (0, \infty) \quad (C1)$$

A sufficient condition to guarantee that $\det(SE+GHE+I_n)$ is not equal to zero is given by inequality C2.

$$\sigma_{\max}(GHE) < \sigma_{\min}(SE+I_n) \quad \text{for all } \omega \in (0, \infty) \quad (C2)$$

or a more conservative condition:

$$\sigma_{\max}(H) < \frac{\sigma_{\min}(SE+I_n)}{\sigma_{\max}(E(SE+I_n)^{-1}G)} \quad \text{for all } \omega \in (0, \infty) \quad (C3)$$

Note that $E(SE+I_n)^{-1}G$ is the transfer function matrix that maps e to the contact force, f . Figure 7 shows the closed-loop system. According to the result of the theorem, H must be chosen such that the size of H is smaller than the reciprocal of the size of the forward loop transfer function, $[E(SE+I_n)^{-1}G]$.

References

- 1) Hogan, N., "Impedance Control: An Approach to Manipulation", ASME Journal of Dynamic Systems, Measurement, and Control, 1985.
- 2) Kazerooni, H., Houpt, P. K., "On The Loop Transfer Recovery", International Journal of Control, Volume 43, Number 3, March 1986.
- 3) Kazerooni, H. "Fundamentals of Robust Compliant Motion for Manipulators", IEEE Journal of Robotics and Automation, N2, V2, June 1986
- 4) Kazerooni, H., "A Design Method for Robust Compliant Motion of Manipulators", IEEE Journal of Robotics and Automation, N2, V2, June 1986.
- 5) Kazerooni, "An Approach to Automated Deburring by Robot Manipulators", ASME Journal of Dynamic Systems, Measurements and Control, December 1986.
- 6) Kazerooni, H., "An Approach to Loop Transfer Recovery using Eigenstructure Assignment". In proceedings of the American Control Conference, June 1985, Boston.
- 7) Kazerooni, H., "An approach to Robotic Deburring", In proceeding of American Control Conference, Seattle, June 1986.
- 8) Kazerooni, H., Guo, J., "Design and Construction of an Active End-Effector", IEEE In proceedings of the IEEE International Conference on Robotics and Automation, Raleigh, North Carolina, April 1987, and also IEEE Journal of Robotics and Automation.
- 9) Lancaster, P., Lambda-Matrices and Vibrating Systems. Pergamon Press, 1966.
- 10) Lehtomaki, N. A., Sandell, N. R., Athans, M., "Robustness Results in Linear-Quadratic Gaussian Based Multivariable Control Designs", IEEE Transaction on Automatic Control AC-26(1):75-92, February, 1981.
- 11) Mason, M. T., "Compliance and Force Control for Computer Controlled Manipulators", IEEE Transaction on Systems, Man, and Cybernetics

- SMC-11(6):418-432, June, 1981.
- 12) Paul, R. P. C., Shimano, B., "Compliance and Control", In Proceedings of the Joint Automatic Control Conference, pages 694-699. San Francisco, 1976.
- 13) Railbert, M. H., Craig, J. J., "Hybrid Position/Force Control of Manipulators", ASME Journal of Dynamic Systems, Measurement, and Control 102:126-133, June, 1981.
- 14) Salisbury, K. J., "Active Stiffness Control of Manipulator in Cartesian Coordinates", In Proceedings of the 19th IEEE Conference on Decision and Control, pages 95-100. IEEE, Albuquerque, New Mexico, December, 1980.
- 15) Slotine, J. J., "The robust Control of of Robot Manipulators", The International Journal of Robotics Research, V4, N2, 1985.
- 16) Vidyasagar, M., "Nonlinear Systems Analysis", Prentice-Hall
- 17) Vidyasagar, M., Desoer, C. A., "Feedback Systems: Input-Output Properties", Academic Press.
- 18) Vidyasagar, M., Spong, M. W., "Robust Nonlinear Control of Robot Manipulators", IEEE Conference on Decision and Control", December 1985.
- 19) Whitney, D.E., "Force-Feedback Control of Manipulator Fine Motions", ASME Journal of Dynamic Systems, Measurement, and Control :91-97, June, 1977.
- 20) Whitney, D. E., "Quasi-static Assembly of Compliantly Supported Rigid Parts", ASME Journal of Dynamic Systems, Measurement, and Control (104):65-77, March, 1982.

1 In this article, "force" implies force and torque and "position" implies position and orientation.

2 The maximum singular value of H is defined as:

$$\sigma_{\max}(H) = \max \frac{\|Hr\|_2}{\|r\|_2}$$

Where $r \neq 0_n$ and $\|\cdot\|_2$ denotes the Euclidean norm.